Current Chemistry Letters 10 (2021) 17–32

Contents lists available at GrowingScience

Current Chemistry Letters

homepage: www.GrowingScience.com

# Synthesis, characterization and biological evaluation of novel octahedral Ru(III) complexes containing pentadentate Schiff base ligands

**Suad A. M. Moubeen[a], M. F. El-Shahat[a], Ayman A. Abdel Aziz[a*] and Attia S. Attia[a]**

[a]*Chemistry Department, Faculty of Science, Ain Shams University, Cairo, Abbasia, 11566, Egypt*

**C H R O N I C L E**

*Article history*:
Received May 15, 2020
Received in revised form
June 26, 2020
Accepted July 13, 2020
Available online
July 14, 2020

*Keywords*:
Ruthenium(III) complexes
Characterization
Antioxidant efficiency
DNA binding
Cytotoxic activity

**A B S T R A C T**

New series of mononuclear octahedral Ru(III) complexes of general formula [$RuL^{1-3}Cl$] (1-3) where L = dianion of Schiff bases namely: 2,2'-(((1E,1'E)-thiophene-2,5-diylbis(methaneylylidene))bis(azaneylylidene))diphenol ($H_2L^1$), 2,2'-(((1E,1'E)-thiophene-2,5-diylbis(methaneylylidene))bis(azaneylylidene))dibenzenethiol ($H_2L^2$) and 2,2'-(((1E,1'E)-thiophene-2,5-diylbis(methaneylyli-dene))bis(azaneylyli-dene))-dibenzoic acid ($H_2L^3$), respectively are synthesized and characterized by different physico-chemical techniques. The results of interaction of complexes with CT-DNA supported that, the Ru (III) complexes bind to DNA via an intercalative mode. The interaction has also been investigated by gel electrophoresis. Interestingly, it was found that all Ru(III) complexes cleave super coiled (SC) pUC19 plasmid DNA efficiently in the absence of an external agent. Further, the antiproliferative activity of the complexes on Human Cervical Cancer Cells (HeLa) and Human Breast Cancer Cells (MCF-7) were evaluated by MTT assay, which revealed that, all the complexes showed more intense inhibition against HeLa and MCF-7 cell lines, particularly Ru(III) complex (3) attenuated the strongest proliferation, allowing its use as chemotherapeutic agent for cancer treatment.



## 1. Introduction

The interaction of DNA with small molecules like metal complexes has been attained as an important link in designing chemotherapeutic agents, to block the replication step in the cell cycle and apply in cancer cell targeting.[1] Stable, inert, and water-soluble transition metal complexes containing spectroscopically active metal center along with different ligands have been examined to identify their affinity for DNA and further evaluated for their anticancer activities with various cell lines.[2-4] The most widely used metal-based clinical cancer therapeutic drugs started with cisplatin and its next-generation compounds show high systemic toxicity and resistance problems.[5,6] For this reason, other metal complexes have attracted attention for the study of in vitro anticancer applications.[7-10] On the other hand, it has been reported that, ruthenium compounds show physicochemical similarities with some of the most efficient anticancer platinum drugs but overcome by its less toxicity, good antiproliferative activity profile in cancer-cell specific targeting properties, convenient rates of ligand exchange, different spectrum of activity, different spectrum of activity, novel mechanism of action and prospect

* Corresponding author. Mobile: +201001300155
E-mail address: aymanaziz31@gmail.com; aymanaziz31@sci.asu.edu.eg (A. A. Aziz)

doi: 10.5267/j.ccl.2020.7.001

of non-cross resistance and have a biologically stable range of oxidation states.[11] Among those ruthenium complexes have emerged as an important area of medical chemistry due to their therapeutic use as antitumor agents, since they present some advantages over platinum complexes currently used in cancer chemotherapy.[12-17] More concretely, ruthenium(III) complexes with Schiff base ligands represent an important group of ruthenium compounds with anticancer activity that is being intensively studied in the last decades.[18,19] Moreover, Free radicals can damage lipids, proteins, and DNA, leading to an increase in cancer rates. Fortunately, antioxidants have the ability to scavenge free radicals.
In the current study, in the light of growing significance for both diagnostic and therapeutic applications in various diseases, we report here the synthesis, characterization, antioxidant scavenging, DNA binding affinity and antiproliferative activity of new ruthenium(III) containing tetradentate Schiff base ligands bearing thiophene moiety.

## 2. Results and Discussion

### *2.1. Elemental analyses and Physical Measurements*

Some physicochemical properties of Ru(III) complexes are given in **Table 1**. The percentage values of C, H, N, S and the physical measurement provided satisfactory results, in with the stoichiometry of 1:1 [Ru(III):Ligand], suggesting a general empirical formula [Ru($L^{1-3}$)Cl] of the coordination compounds. The solubility tests showed that, the complexes were soluble in water and polar organic solvents. Molar conductance values of complexes in DMSO measured at room temperature were 16.1, 19.5 and 12.9 $\Omega^{-1}cm^2mol^{-1}$ for complexes 1, 2 and 3, respectively. Those values reflect the non-electrolytic nature of the complexes.[20]

**Table 1.** Molecular formula, Elemental analysis and UV-visible spectral analyses of Ru(III) complexes (1-3).

| Complex | Molecular formula | (Calculated) Found (%) | | | | | | UV-Vis, $\lambda_{max}$ (nm) |
|---|---|---|---|---|---|---|---|---|
| | | C | H | N | S | Cl | Ru | |
| [Ru($L^1$)Cl] **(1)** | [$RuC_{18}H_{12}N_2O_2SCl$] | (47.32) 46.99 | (2.65) 2.57 | (6.13) 6.11 | (7.02) 7.00 | (7.76) 7.66 | (22.12) 22.01 | 261[a], 324[b], 440[c] |
| [Ru($L^2$)Cl] **(2)** | [$RuC_{18}H_{12}N_2S_3Cl$] | (44.21) 43.99 | (2.47) 2.42 | (5.73) 5.68 | (19.67) 19.53 | (7.25) 7.17 | (20.67) 20.39 | 278[a], 316[b], 395[c] |
| [Ru($L^3$)Cl] **(3)** | [$RuC_{20}H_{12}N_2SO_4Cl$] | (46.83) 46.71 | (2.36) 2.32 | (5.46) 5.38 | (6.25) 6.01 | (6.91) 6.88 | (19.71) 19.66 | 258[a], 333[b], 398[c] |

a π-π* transition; b n-π* transition; c MLCT

### *2.2. Infrared Spectra*

In order to provide important information about the coordination mode of the ligands to the Ru(III) ion, infrared spectra of the reported ligands and their Ru(III) complexes were recorded in the 4000-400 $cm^{-1}$ region using KBr pellets. In the free Schiff base $H_2L^1$, the υ(OH) absorption observed as a broad medium intensity band around 3130-3423 $cm^{-1}$ which give an indication of the presence of a strongly hydrogen bonded related to one Ar-OH group.[21] Additionally, an intense and sharp absorption band was observed at 3357 $cm^{-1}$ which was assigned to non-hydrogen bonding OH group in the free ligand. Upon complexation with Ru(III) ion to form complex (1), those ligand bands were disappeared, indicating deprotonation prior to the coordination through the phenolic oxygen atoms. The involvement of the phenolic oxygen atoms in coordination with Ru(III) ion was further substantiated by frequency lowering in the medium band ascribed to υ(C-O) from 1297 $cm^{-1}$ in the free parent ligand to 1285 $cm^{-1}$ in complex.[23] In the low frequency region of the Ru(III) complex (1), low intensity band at 515 $cm^{-1}$ was designate to the formation of ν(Ru–O) vibrations, which further support the coordination of the Schiff bases to the Ru(III) center through the phenolic oxygen.[23] The FT-IR spectrum of the second Schiff base $H_2L^2$, didn't give an indication of the presence of the thiol (S-H) group, which may be arises from intramolecular N···H—S hydrogen bonds leading a broad medium intensity band at 3328 $cm^{-1}$

due to $HN^+$ moiety.[24] Furthermore, FT-IR spectrum of $H_2L^2$ displayed a strong band at 1607 $cm^{-1}$ relating to $\nu_{C=N}$ stretching frequency, which exhibited a negative shift to 1604 $cm^{-1}$ after chelation to Ru(III) ion, in accordance with participation of the azomethine nitrogen in coordination.[25] With respect to the free Schiff base ligand $H_2L^3$, a broad and medium intensity band at 3426 $cm^{-1}$ which was attributed to the intermolecular hydrogen bond due to carboxylic OH groups of the Schiff base disappeared upon chelation, this band with Ru(III) ion. Moreover, in the free Schiff base ligand $H_2L^3$. $\upsilon$(C=O) frequency of the carboxyl group was seen as a band around 1700 $cm^{-1}$ was absent in upon chelation with Ru(III) ion). On contrary, upon complexation with Ru(III) ion, two band were recorded at 1617 $cm^{-1}$ and 1325 $cm^{-1}$ due to $_{asym}(CO_2^-)$ and $\nu_{sym}$ $(CO_2^-)$ vibrations, respectively. The difference between $\upsilon_{asym}$ and $\upsilon_{sym}$ vibrations ($\Delta = \nu_{asym(COO-)} - \nu_{sym(COO-)}$) gave a is a clear evidence of the unidentate coordination of the carboxyl group with the free carbonyl group.[26] This fact was further confirmed by the presence of new band at 516 $cm^{-1}$ assignable to $\nu$(Ru–O).[27] IR spectra of all ligands show a sharp band at the region 1607-1613 $cm^{-1}$ which, is characteristic of the azomethine $\nu$(C=N) stretching. In Ru(III) complexes (1-3), this band was shifted to 1591-1609 $cm^{-1}$, indicating coordination of the Schiff bases through nitrogen of azomethine group to Ru(III).[28] Furthermore, such mode of chelation was supported by the appearance of a new non-ligand weak band in the range of 418-491 $cm^{-1}$ which assigned to M-N stretching.[29] Thiophene C–S stretching observed at 739 $cm^{-1}$, at 722 $cm^{-1}$ and at 732 $cm^{-1}$ in the IR spectra of $H_2L^1$, $H_2L^2$ and $H_2L^3$, respectively. In all complexes, this band frequencies were shifted to 743 $cm^{-1}$, 732 $cm^{-1}$ and 735 $cm^{-1}$ respectively, confirming the involvement of the thiophene sulfur in complex formation.[30] The FT-IR spectra of the ligands and their complexes are delineated in **Figs. S1-S6**.

*2.3. Mass Spectra*

The mass spectra of the metal complexes were recorded in DMSO solution. The mass spectra of the complexes are used to correlate their stoichiometric composition. The mass spectra of Ru(III) complexes (**Fig. S7-S9**) confirmed the proposed structure. The mass spectra of Ru(III) complexes were observed at m/z = 456.81, 489.00 and 512.88, respectively, which are in good agreement with their molecular weights.

*2.4. Magnetic Susceptibility and EPR Spectra*

The effective magnetic moment values were calculated from the equation: $\mu_{eff} = 2.83\sqrt{\chi_M T}$ where $\mu_{eff}$ is the effective magnetic moment, $\chi_M$ is the magnetic susceptibility per one Ru(III) center, and T is the absolute temperature. The ruthenium(III) complex showed magnetic moment values at 1.79, 1.81 and 1.84 B.M, respectively, which reflect the presence of one unpaired d electron leading to +3 and which is consistent with octahedral geometry. EPR spectra of powdered complexes were recorded at room temperature. The complexes showed no indication for any hyperfine interaction of nuclei with magnetic moments viz., ruthenium. All of the complexes exhibit a single isotropic resonance with 'g' values in the range 2.0072-2.01163 (**Fig. 1**). Such isotropic lines are usually observed either due to the intermolecular spin exchange which can broaden the lines or due to occupancy of the unpaired electron in a degenerate orbital. However, similar chloro complexes[31] showed a single line due to the presence of one unpaired electron in a low-spin state with a degenerate $d_{xz}$, $d_{yz}$ ground state indicating Jahn-Teller instability,[30] resulting in an averaged single 'g' value. The position of the lines and the nature of the EPR spectra of all the complexes suggest an almost perfect octahedral environment around the ruthenium ion in the complexes.[32]

*2.5. Electronic Spectra*

As a very helpful technique for concluding the stereochemistry of metal ion complexes, the UV-Vis absorption spectra of complexes solutions were record at room temperature in 5% DMSO in Tris buffer (pH 7.2) solution in region 200-800 nm (**Fig. 2**). The spectra of the complexes exhibit the

characteristic transitions at 258-278 nm and 316-333 nm corresponding to intramolecular π→π∗ and n→π∗ transitions, respectively. Additionally, all ruthenium complexes display bands display strong absorption band in region at 395-441 nm, respectively, due to the d(Ru)→π* (ligand) MLCT transitions.[33] This MLCT transition is particularly important as it is perturbed when the complex interacts with DNA, providing a spectroscopic probe.[34]

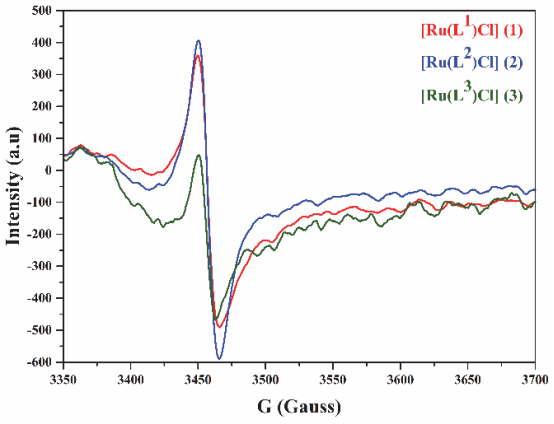


**Fig.1.** EPR spectra of powdered Ru(III) complexes at room temperature

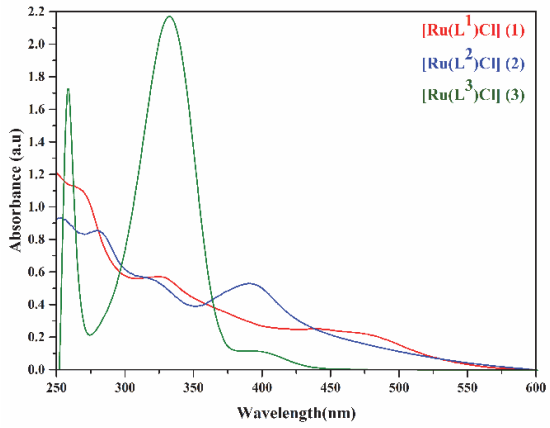


**Fig. 2.** UV-Vis. spectra of Ru(III) complexes (1-3) in 5% DMSO in Tris buffer (pH 7.2)

Based on the analytical, spectroscopic data (FT-IR, UV-Vis, EPR, ESI-mass), the following tentative mononuclear octahedral structure has been proposed for all of the new complexes (**Fig. 3**).

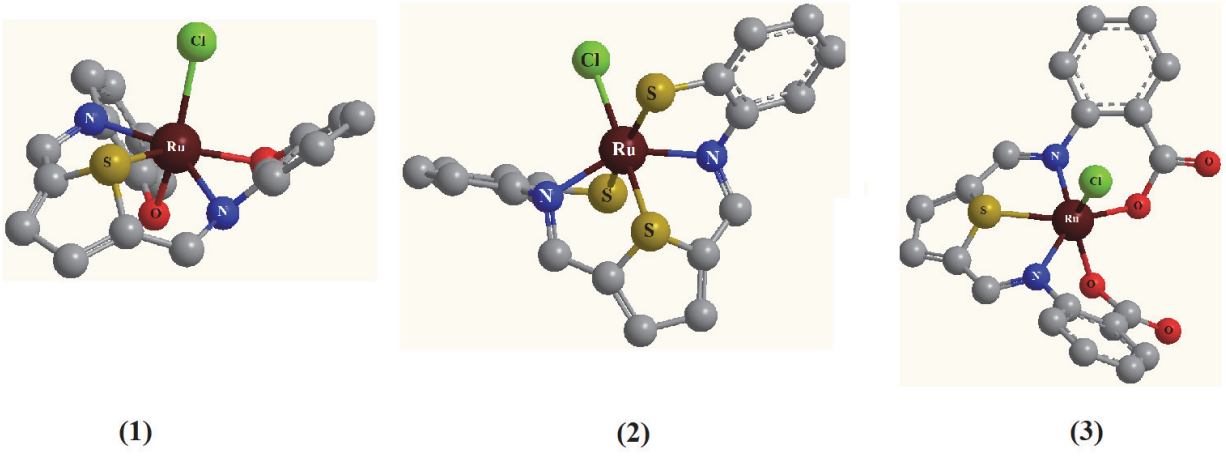


**Fig. 3.** Optimized proposed structure of mononuclear octahedral Ru(III) complexes (1-3)

*2.6.* Scavenging Activities

Oxidative reactions of biological molecules induce a variety of pathological events such as cellular injury and aging process, and these damaging events are caused by free radicals.[35] Therefore, to prevent free radical damage in the body, it is important to administer drugs that may be rich in antioxidants. Antioxidant activities of Ru(III) complexes (1-3) were ascertained by DPPH stable commercially available free radical scavenging assay method using ascorbic acid as reference. This method based on the ability of the antioxidant to donate its electron to DPPH, which in turn upon reduction by an antioxidant, the color of, (DPPH) to change from purple to yellow. The results have shown that Ru(III) complexes exhibited potent scavenging capacity for all the concentrations used (**Fig. 4**), which may be due proton from the test samples were transferred to DPPH, converting it into the corresponding hydrazine form.[36] Moreover, as shown **Fig. 5**, in terms of the $IC_{50}$ values, the compounds showed antioxidant capacity according to the following rank 3 > 1 > 2.

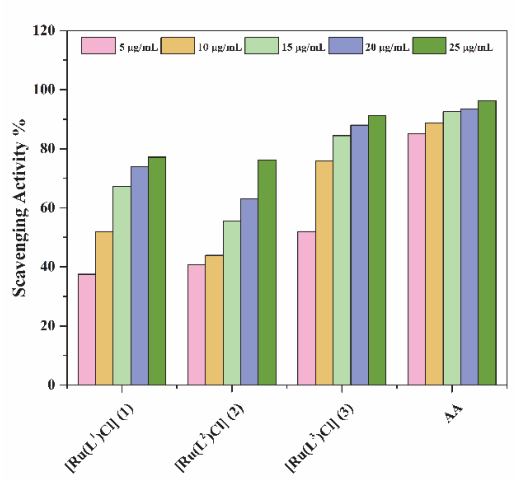


**Fig. 4.** Antioxidant activity of Ru(III) complexes (1-3) and ascorbic acid (AA) against DPPH

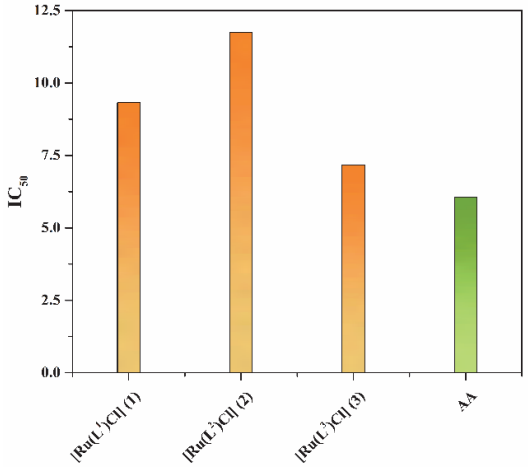


**Fig. 5.** Radical scavenging activity of Ru(III) complexes (1-3) in terms of $IC_{50}$ value (50% inhibition)

## *2.7. DNA Binding Affinity*

### *2.7.1. UV-Vis Absorption Interaction Studies*

Upon addition of increasing concentrations of CT-DNA to Ru(III) with fixed concentration (20 µM), the absorption bands corresponding to the intraligands and MLCT displayed hypochromicity and bathochromicity (red shift) (**Fig. 6**). A comparison of the magnitude of hypochromism and bathochromicity are in the order of complexes 3 > 1 > 2. The observed spectral behavior obviously ruled out intercalative binding of the investigated compounds to DNA. As described in the experimental procedure, in order to quantify the extent of DNA binding and as a measure of the binding strength,[37] the intrinsic binding constant ($K_b$) of Ru(III) complexes were determined and it is found to be $2.13 \times 10^5$ $M^{-1}$ (1), $1.42 \times 10^5$ $M^{-1}$ (2) and $2.24 \times 10^5$ (3), respectively (**Fig. 6 Insets**). These $K_b$ values follows the order 3 > 1 > 2. The $K_b$ values of Ru(III) complexes indicate the binding affinity between the complex and DNA is close to that of classical intercalators (e.g., EtBr -DNA, ~$10^6$ $M^{-1}$).[58] The intrinsic binding constant values ($K_b$, $M^{-1}$) of all Ru(III)complexes (1-3) with CT-DNA, the hyperchromatism extent (H%) and red shift (Δλ, nm) have been summarized in **Table 2**.

### *2.7.2. Competitive Binding Fluorescence Quenching Measurements*

Further, to support the competitive binding of Ru(III) complexes (1-3) to DNA via intercalation, fluorescence emission quenching experiments were performed. EtBr (ethidium bromide) alone show minimal fluorescence and the fluorescence was enhanced greatly with the gradual addition of CT-DNA until a maximum fluorescence was achieved due to the formation of an intercalative DNA-EtBr adduct. The displacement evaluation of common DNA probe, EtBr was used to measure the relative binding of the investigated compounds to CT-DNA. As seen in **Fig. 7**, upon addition of increasing amounts of the Schiff bases and the complexes to DNA pre-treated with EtBr, a significant decrease in the fluorescence intensity was observed, giving a clear evidence for replacement of the EtBr by the investigated compounds. To further validate the binding strength of all the tested compounds, the $K_{SV}$ values obtained from the plot of $I_0/I$ versus [Ru(III) complex] were $3.14 \times 10^5$ $M^{-1}$ , $4.92 \times 10^5$ $M^{-1}$, and $5.31 \times 10^5$ $M^{-1}$ corresponding to complex (1), complex (2) and complex (3) respectively (**Fig. 7 Insets**). Hence, the results give clear evidence that the binding strength of the Schiff bases and their Ru(III) complexes were in good agreement with the binding constants derived from absorption spectra measurements and suggest that the interaction of both the complexes with CT-DNA via intercalative mode. The binding extent was further deeply insight by calculation of the apparent DNA binding values

($K_{app}$). The apparent binding coefficients are showed in **Table 2**. The $K_{app}$ values obtained here for CT-DNA are higher than those reported for classical intercalator (EtBr-DNA, $3.3 \times 10^5$ $M^{-1}$ in 50 mM Tris-HCl/1.0 M NaCl buffer, pH 7.5).[58]

**Table 2.** The Physical binding data of Ru(III) complexes with CT-DNA.

| Complex | $\lambda_{max}$ | | $\Delta\lambda$ (nm) | H %[a] | $K_b$ ($M^{-1}$)[b] | $K_{SV}$ ($M^{-1}$)[c] | $K_{app}$ ($M^{-1}$)[d] |
|---|---|---|---|---|---|---|---|
| | Free | Bound | | | | | |
| [Ru($L^1$)Cl] **(1)** | 440 | 448 | 8 | 17.7 | $2.13\times10^5$ | $4.92 \times 10^5$ | $6.14 \times 10^5$ |
| [Ru($L^2$)Cl] **(2)** | 395 | 400 | 5 | 11.6 | $1.42 \times 10^5$ | $3.14 \times 10^5$ | $5.67 \times 10^5$ |
| [Ru($L^3$)Cl] **(3)** | 398 | 409 | 11 | 24.7 | $2.24\times10^5$ | $5.31 \times 10^5$ | $6.82 \times 10^5$ |

a: Percentage of hypochromism; b: Binding constant; c Stern- Volmer constant; d Kapp Apparent binding constant

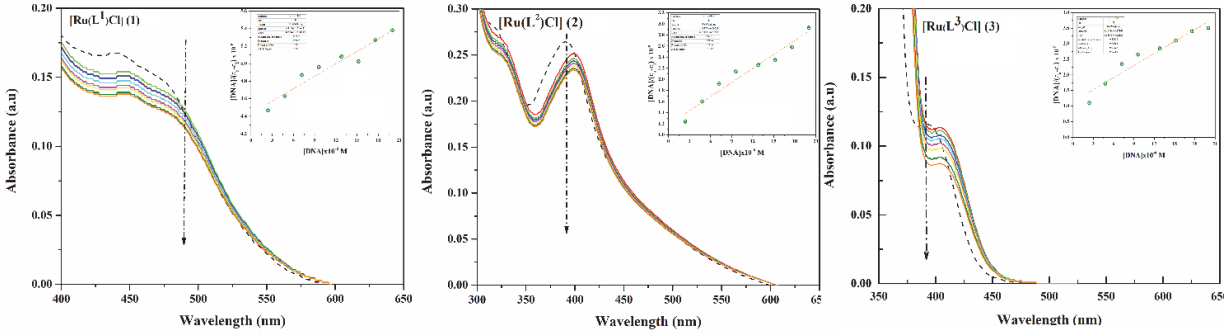


**Fig. 6.** Absorption spectra of [Ru($L^{1-3}$)Cl] complexes (1-3) upon the increasing of CT-DNA concentration (0-50 μM). Arrow indicates changes in the emission intensity upon addition of different complex concentration. Arrow indicates changes in optical density upon addition of different complex concentration. Inset: Linear plot of [CT-DNA]/($\varepsilon_a$ - $\varepsilon_f$) vs [CT-DNA] for the calculation of the intrinsic binding constant, $K_b$

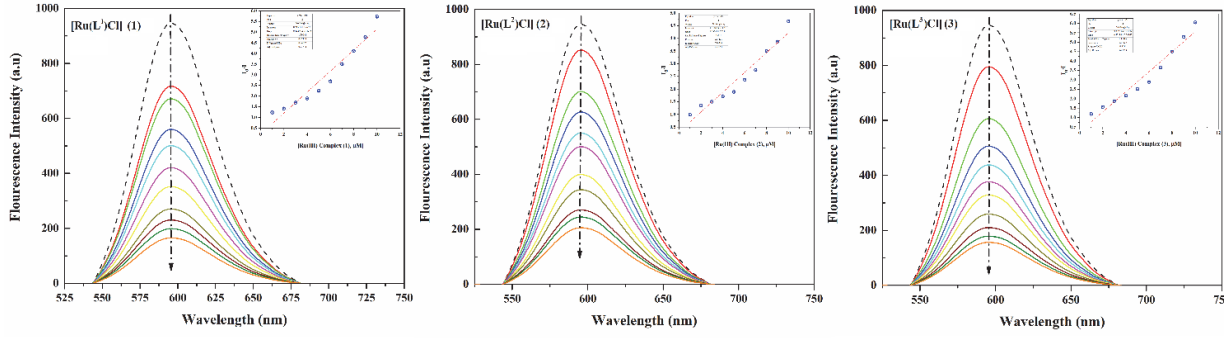


**Fig. 7.** Emission spectra of EtBr bound to the CT-DNA, Black dashed line), in the presence (other colored lines) of 2.4-20 μM [Ru($L^{1-3}$)Cl] complexes (1-3). Arrow indicates changes in the emission intensity upon addition of different complex concentration. (Inset: Stern-Volmer plot of the EtBr-DNA. [CT-DNA] = 10 μM, [EtBr] = 10 μM. Stern-Volmer plots for the calculation of the quenching constant, $K_{SV}$

### *2.7.3. Viscosity Measurements*

Although optical photophysical methods are employed to offer essential information about the binding monitor the binding mode of Ru(III) complex with the DNA, they are lacking evidences to support an intercalative binding model.[39] Viscosity measurements as a simple hydrodynamic technique are preferred as the confirmation tests in the absence of crystallographic data.[40] To elucidate the nature of DNA binding of the novel complexes, viscosity measurements were carried out to examine the effect of the complexes (1-3) on the relative specific viscosity of the CT-DNA. The changes in the relative specific viscosities of CT-DNA in presence and absence of Ru(III) complexes (1-3) were plotted against [Complex]/[CT-DNA] (**Fig. 8**). As illustrated in **Fig. 8**, the recorded output data manifested that the relative viscosity of CT-DNA increases with in concentration intension of investigated compounds, which is similar to that of typical classical intercalator, ethidium bromide.[41] Such an

intension in viscosity is consistent with that, the complexes classically intercalate between the double-stranded DNA, that causes the unwinding and lengthening of the said DNA to accommodate the bound complex, leading to the increase of DNA viscosity.[42] The increase in the viscosity implies the metal complex intercalation between the DNA base pairs that causes the unwinding and lengthening of the said DNA. Additionally, the obtained results showed that Ru(III) complexes are good metallointercalators, with complex (3) being highly effective than the others.

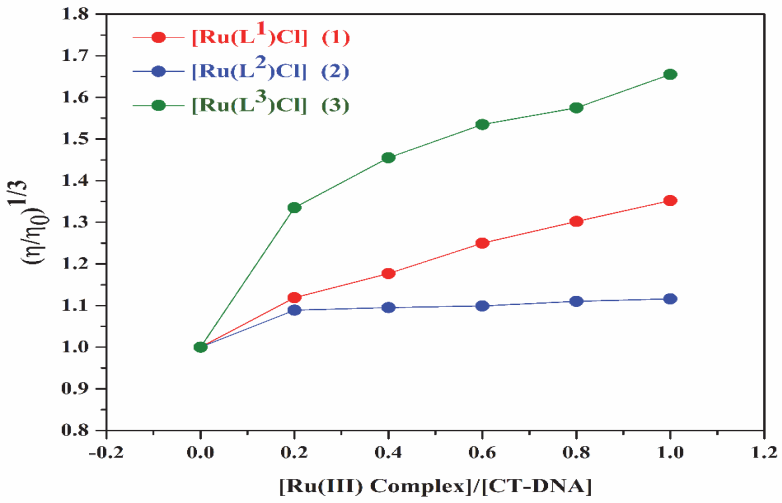


**Fig. 8.** Relative viscosity of CT-DNA $(\eta/\eta_o)^{1/3}$ in buffer solution (20 mM Tris-HCl, 20 mM NaCl at pH 7.2) in the presence of Ru(III) complexes 1-3 at increasing amounts of [Ru(III) complex]/[CT-DNA]

*2.8 DNA Cleavage Activity*

The study on the cleavage capacity of transition metal complex to DNA is considerably interesting as it can contribute to understanding the toxicity mechanism of them and to develop novel artificial nuclease. DNA cleavage is controlled by relaxation of super coiled circular form of pUC19 DNA into nicked circular form and linear form. When circular plasmid DNA is conducted by electrophoresis the fastest migration will be observed for the supercoiled form (Form I). If one strand is cleaved, the supercoils will relax to produce a slowed moving open circular form (Form II).[43] The cleaving efficacy of Ru(III) complexes (1-3) has been assessed by their ability to convert supercoiled pUC19 DNA from form I to form II by agarose gel electrophoresis. The cleavage patterns of synthesized complexes are shown in **Fig. 9**. As shown in cleavage patterns of synthesized Ru(III) complexes (1-3), no distinct DNA cleavage was observed in absence of the complex (control, lane 1); however, with fixed concentration of the complexes, cleave SC (Form I) DNA into nicked circular (NC) (Form II) DNA. Hence, in presence of complexes, DNA efficiently cleaved into nicked form in the absence of an external agent.[44] Further it is observed that Ru(III) complex (3) promote the cleavage of supercoiled pBR322 DNA more efficiently than other complexes. Additionally, the amount of helical unwinding induced by the complex bound to SC DNA provides evidence for the intercalation mode of interaction between the complexes and DNA. The DNA cleavage activity of the complexes (1-3) can be estimated from the percentage of cleavage (**Table 3**).

**Table 3.** Self-activated cleavage data of SC pUC19 DNA (10 μM) by Ru(III) complexes (**1-3**); 30 μM) for an incubation time of 1 h.

| Lane No | DNA control | Percentage of cleavage (%) | |
|---|---|---|---|
| | | SC (I) | NC (II) |
| **1** | DNA | 100 | 0 |
| **2** | DNA + [Ru($L^1$)Cl] **(1)** | 62.13 | 37.78 |
| **3** | DNA + [Ru($L^2$)Cl] **(2)** | 66.17 | 33.83 |
| **4** | DNA + [Ru($L^3$)Cl] **(3)** | 55.75 | 44.25 |

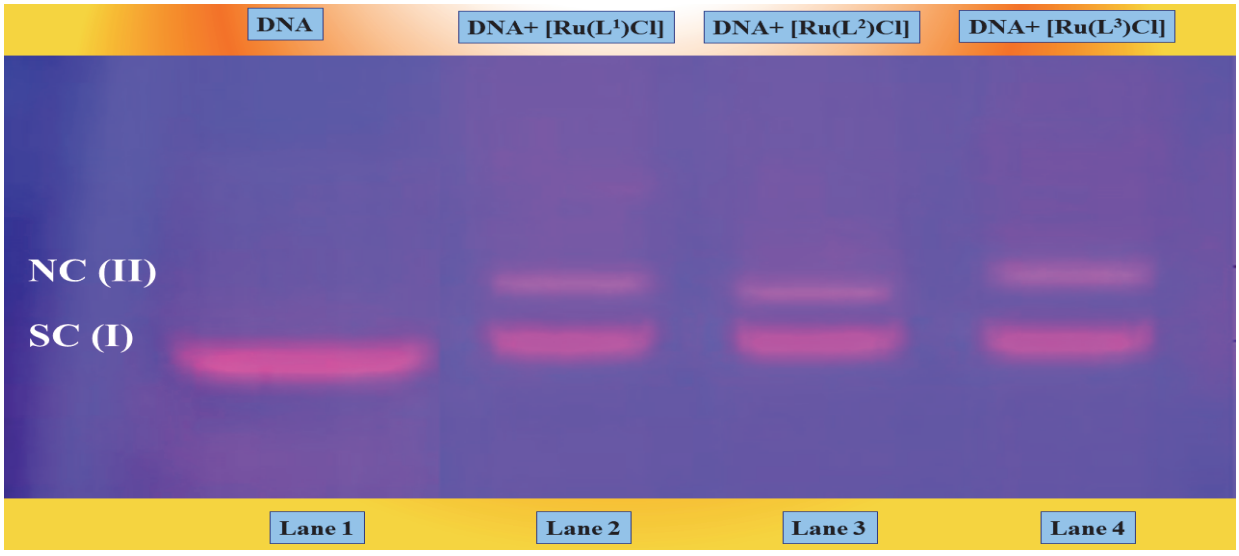


**Fig. 9.** Gel electrophoresis diagram of pUC19 DNA (10 µM) by Ru(III) complexes (30 µM) in a in 50 mM Tris-HCl/50 mM NaCl buffer (pH 7.2) and 37 ºC with an incubation time of 1 h. lane 1, DNA control; lane 2, DNA + [Ru($L^1$)Cl] (1); lane 3, DNA + [Ru($L^2$)Cl] (2); lane 4, DNA + [Ru($L^3$)Cl] (3). Forms SC and NC are supercoiled and nicked circular DNA, respectively.

*2.9. In vitro* Antiproliferative Activity

To evaluate cancer chemotherapeutic potential, ability of Ru(III) complexes (1-3) to kill two human Cervical Cancer Cells (HeLa) and Human Breast Cancer Cells (MCF-7) were assessed by using a 3-(4,5-dimethylthiazol-2-yl)-2,5-diphenyl-tetrazolium bromide (MTT) assay for cell viability **(Fig. 10 and Fig. 11**). The results revealed that, the complexes have strong antiproliferative effect against the two types of cancer cells and the inhibition effects were enhanced by increasing the concentration of complexes. As a measure of therapeutic potential, the inhibitory concentration of the tested compounds and standard drug (*cis*-platin) required for 50% cell inhibition ($IC_{50}$) of the cells are shown in **Fig. 12**. The $IC_{50}$ values have shown that complex (3) exhibited a higher inhibitory effect and the $IC_{50}$ is very close to the value of *cis*-platin. The cytotoxicity results are in good agreement with the DNA binding ability of the complexes.[45,46] The study of morphology of cancer cells belongs to the elusive areas of human endeavor where objective evidence has not kept pace with subjective recognition of patterns. A cancer cell is usually morphologically abnormal, i.e., it perceptibly differs from normal cells of similar anatomic origin. In some cases, the degree of cell abnormality is such that an almost instantaneous microscopic recognition of cancer is possible. The morphology examinations also show that the proliferation of the cells is significant inhibited, and the cells exhibit morphological changes such as cell shrinkage and cell detachment (**Fig. 13**).

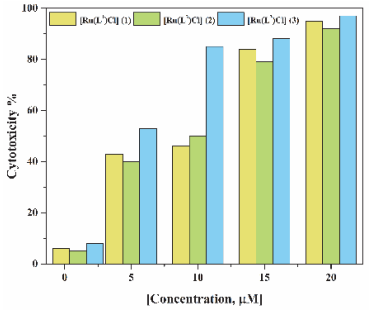


**Fig. 10.** The cytotoxicity of Ru(III) complexes (1-3) against Hela human cervical cancer cells (HeLa)

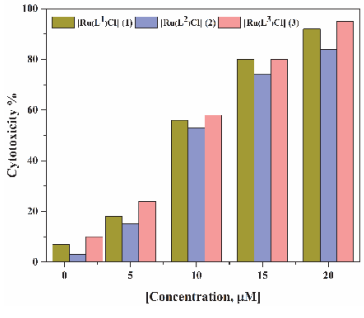


**Fig. 11.** The cytotoxicity of Ru(III) complexes (1-3) against human breast cancer Cells (MCF-7)

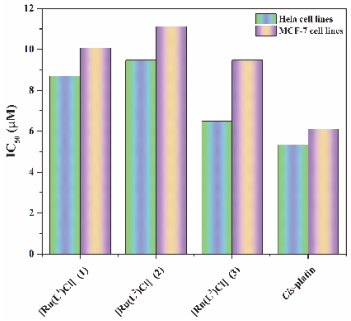


**Fig. 12.** The antiproliferative activity *in vitro* expressed as $IC_{50}$ (µM) values of Ru(III) complexes (1-3) and cisplatin against Hela and

MCF-7 human tumor cell lines

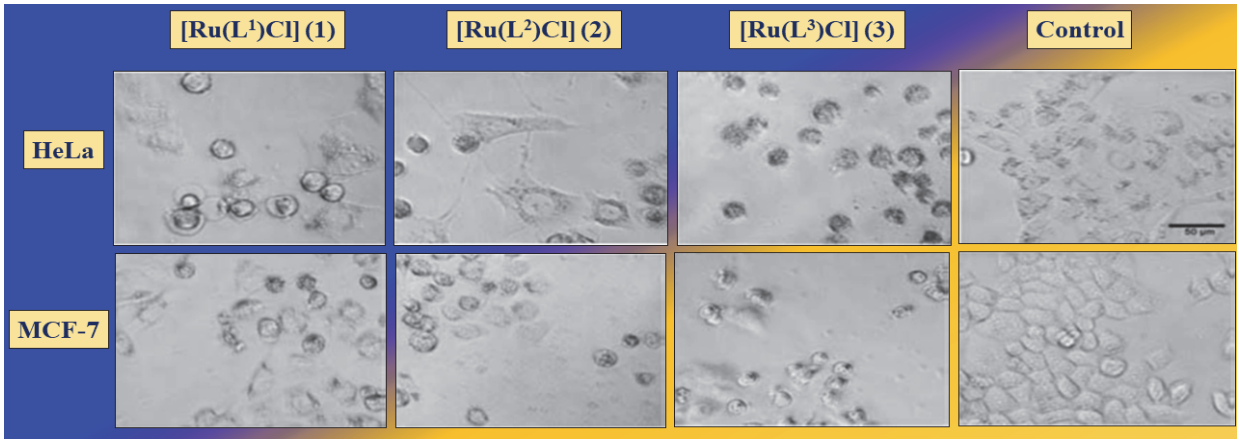


**Fig. 13.** Phase-contrast micrographs of HeLa and MCF-7 cells treated with Ru(III) complexes (1-3)

## 3. Conclusions

In summary, we report on the synthesis and characterization of mononuclear Ru(III) complexes have been achieved, and it is observed that all the complexes acquired an octahedral geometry with 1:1 ruthenium to ligand ratio. The characterization of all complexes was accomplished by a series of spectroscopic techniques, including UV-Vis., FT-IR, ESI-MS, molar conductance and magnetic susceptibility techniques. In all complexes, the ligands are bound to the metal in a pentadentate fashion. The scavenging activity of the compounds towards DPPH radical was noteworthy. The scavenging activity of complex (3) was significantly high and comparable to the reference compounds. The interaction of compounds with CT DNA was investigated by diverse techniques. DNA binding studies have revealed that all the complexes are capable of binding with DNA via intercalative mode. In vitro study of the cytotoxicity of the complexes on HeLa and MCF-7 show good antitumor activity against selected cell lines.

## 4. Experimental

### *4.1. Materials and Methods*

2,5-Thiophenedicarboxaldehyde, 2-aminophenol, 2-aminothiphenol, 2-aminobenzoic acid and $RuCl_3.xH_2O$ were purchased from Sigma-Aldrich (Saint Louis, MO 63103 USA). All chemicals and solvents were of analytical grade, supplied from Merck (Darmstadt, Germany) and used without further purification. Micro analyses (C, H, N) were performed on Perkin-Elmer 2400 CHN elemental analyzer. Cl content in complex was determined by gravimetric method.[47] The Sulphur content was determined by oxygen flask method.[48] FT-IR spectra were recorded on a Unicam-Mattson 1000 FT-IR in the region of 4000-400 $cm^{-1}$ using KBr pellets. Mass spectra were performed in the positive ion mode on a liquid chromatography-ion trap mass spectrometer (LCQ 83 Fleet, Thermo Fisher Instruments Limited, USA) using the ESI technique. Molar conductivities were measured in 5% DMSO-Tris buffer (pH 7.2) solution, concentration of $10^{-3}$ M, at 25 °C on YSE conductance meter model 32. UV-visible spectra were measured at 25 °C in 5% DMSO-Tris buffer (pH 7.2) (concentration of $1 \times 10^{-5}$ M) using Shimadzu UV-Vis 1800 spectrophotometer. Fluorescence measurements were carried out on a Jenway 6270 Fluorimeter, using Pulsed Xenon Lamp as an excitation source. Magnetic susceptibility measurements at room temperature of powdered samples were recorded on a Johnson-Matthey DG8 5HJ balance, by Gouy method and corrected for diamagnetism of the component using Pascal's constants.[49]

*4.2. Synthesis of Ligands*

The ligands were synthesized using a conventional method as previously reported in the literature.[50-52] 0.7 g, (5.0 mmol) of 2,5-thiophenedicarboxaldehyde dissolved in 20 mL of a hot methanolic solution was slowly added to the appropriate amine (10 mmol). dissolved in hot methanolic solution (20 ml). After completion of addition, the mixture was allowed to stir, refluxed on a water for ca 2 h and then allowed to cool at room temperature. The yellow crude product was recrystallized from warm methanol. The products were dried in vacuum over anhydrous $CaCl_2$ overnight to give analytically pure products in good yields. The synthetic route to $H_2L^{1-3}$ is shown in **Scheme 1**.

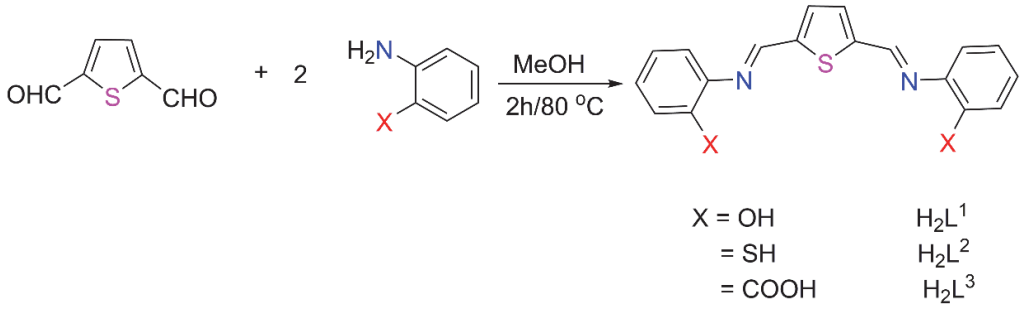


**Scheme 1.** Synthetic route of the Schiff base ligands to $H_2L^{1-3}$

*4.3. Synthetic Procedure for Complexes (1-3)*

All the new complexes were synthesized using the general procedure in **Scheme 2**. To an ethanolic solution (20 mL) of $RuCl_3.xH_2O$, (0.20743 g, 1.0 mmol), 1.0 mmol of the appropriate Schiff base (0.32238, 0.35451g, 0.378.4g ) was added. The mixture was stirred and refluxed for ca 3 h and the solution was concentrated to ca. 5 mL. The solid were isolated by filtration, washed with a small amount of cold methanol (ca. 2 mL), hot petroleum ether 40-60 °C, and recrystallized from $CH_2Cl_2$ and dried under vacuum, over silica gel. The yields were within the range of 75-91 %.

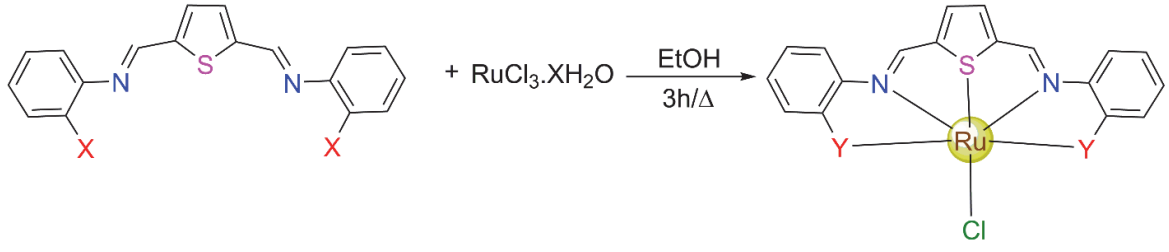


**Scheme 2.** Synthetic route for Ru(III) complexes (1-3)

*4.4. Estimation of Ru Content*

A spectrophotometric method was used for determination of Ru(III) content in complexes using 2-hydroxy-3-methoxy benzaldehyde thiosemicarbazone (HMBATC).[53] Known weight of the Ru complex containing Ru(III) in the range of 0.50 - 8.10 µg/mL was dissolved in nitric acid and making

it to a standard volume. In a 10 mL standard flask, 5 mL acetate buffer solution (pH 2.5), 1.0 mL of Ru(III) solution and 1.0 mL of HMBATSC ($1 \times 10^{-2}$ M) were taken and the volume was made up to the mark with doubly distilled water. The absorbance was measured at 390 nm against the reagent blank. The calibration curve was constructed by plotting the absorbance against the amount of Ru(III) in the range of 0.50–8.10 μg $ml^{-1}$. The calibration graph follows the straight-line equation Y = a c + b; where c was the concentration of the solution, Y was measured absorbance or peak height and a and b were constants.

*4.5. Antioxidant Activity Evaluation*

To evaluate the radical scavenging activity of these compounds, DPPH (2,2-diphenyl-1-picrylhydrazyl) assay method was used to test the free radical scavenging activity of the samples.[54] The evaluation of antioxidant activity assay based on the conversion of DPPH into 1,1-diphenyl-2-picrylhydrazine. For the quantitative estimation of scavenging activity, stock solution of 1 mM DPPH was prepared in methanol and the solutions of ascorbic acid and different concentrations of test compounds (1.0 mg/mL). In different test tubes, 1 mL of each sample solution (10-50 μM), 3 mL of DPPH solution (0.1 mM) was added and the mixture was shaken vigorously for ~ 5 min. After 20 min of incubation in dark room, the absorbance of test solutions was recorded at 517 nm (purple color with $\varepsilon = 8.32 \times 10^3$ L $mol^{-1}cm^{-1}$) at room temperature. The control experiment was carried out as above without the test samples. Ascorbic acid was used as standard whereas DPPH was used as positive control and DMSO was used as negative control. The reduction of DPPH was calculated relative to the measured absorbance of control. The DPPH radical scavenging activity of the compounds was calculated using Eq.(1):

$$\text{Radical scavenging activity \%} = \frac{A_C - A_S}{A_C} \times 100, \quad (1)$$

where $A_C$ is the control absorbance (blank) and $A_S$ is the sample absorbance. All the analyses were made in in triplicate for each and the results were compared with control.

*4.6. DNA Binding Studies*

Calf thymus-DNA (Sigma) was used as received. The stock solution of CT-DNA was prepared by dissolving appropriate amount of DNA in (hydroxymethyl)aminomethane-HCl (Tris-HCl) buffer (20 mM Tris-HCl, 20 mM NaCl, pH 7.2) using milliQ water by gentle stirring at room temperature and stored at 0-4 °C and used after no more than 4 days. The ratio of the UV absorbance at 260 and 280 nm ($A_{260}/A_{280}$) of DNA solution was checked to be ca. 1.8-1.9:1, indicating that DNA was adequately free from protein contamination. The concentration of CT-DNA per nucleotide phosphate [NP] was determined from its absorbance at 260 nm using $\varepsilon_{260}$ = 6600 L $mol^{-1}cm^{-1}$.[55] Complex solutions were prepared in 5% DMSO in Tris buffer for all DNA studies.

*4.6.1. UV-Visible Absorption Spectroscopy Titration*

Electronic absorption spectral titration experiments were performed using a fixed concentration of the investigated complexes (10 μM) to which variable DNA concentrations ranging from 2.4 to 20 μM were added. Before recording the absorption spectra, the solutions were allowed to incubate for 5 min. In case of Ru(III) complexes, the absorption titrations were performed by monitoring the changes of absorption in the MLCT band with increasing concentration of DNA. All observed absorption spectra were corrected by addition of equal amounts of DNA to reference buffer solutions to eliminate the absorbance of DNA itself. Quantitative DNA-binding affinities of Ru(III) complexes are estimated by calculating their intrinsic binding constants ($K_b$) with CT-DNA using the using modified Wolfe-Shimer Eq. (2):[56]

$$\frac{[DNA]}{(\varepsilon_a - \varepsilon_f)} = \frac{1}{K_b(\varepsilon_b - \varepsilon_f)} + \frac{[DNA]}{(\varepsilon_b - \varepsilon_f)} \quad (2)$$

where [CT-DNA] is the concentration of CT-DNA in base pairs, $\varepsilon_a$ is the molar extinction coefficient of the complex at a given DNA concentration, $\varepsilon_f$ is the molar extinction coefficient of the complex in free solution and $\varepsilon_b$ is the molar extinction coefficient of the complex when fully bound to DNA. A plot of [DNA]/($\varepsilon_a$- $\varepsilon_f$) versus [DNA] gave a slope of 1/($\varepsilon_b$ - $\varepsilon_f$) and a Y intercept equal to 1/$K_b$($\varepsilon_b$ - $\varepsilon_f$); $K_b$ is the ratio of the slope to the Y intercept.

*4.6.2. Fluorescence Quenching Measurements*

Fluorescence property has not been observed for the complexes at room temperature in solution or in the presence of CT DNA, so the binding of the complexes with DNA could not be directly predicted through the emission spectra. Hence, competitive binding study was done to understand the mode of DNA interaction with the complexes.[57] The competitive fluorescence titration studies of Ru(III) complexes (1-3) with ethidium bromide (EtBr) solution were carried out by the addition of the varying concentration (2.4-20 μM) of the tested complexes solution to EtBr-bound CT-DNA solution in Tris-HCl buffer. The fluorescence intensity was measured at 596 nm ($\lambda_{ex}$ 520 nm) after incubation for ~ 10 min at room temperature. The measurements were repeated until there was no spectral change for at least three times. Fluorescence quenching data was further analyzed by Stern-Volmer eq. (3):[58]

$$\frac{I_o}{I} = 1 + K_{SV}\,[\text{Ru (III) complex}] \quad (3)$$

where $I_o$ and I are the emission intensity in the absence and presence of Ru(III) complexes. $K_{sv}$ is the Stern-Volmer quenching constant, which is obtained as a slope from the plot of $I_o$/I versus [Ru(III) complex]. To further elucidate the binding extent, apparent DNA binding values (Kapp) were analyzed by eq (4).[59]

$$K_{EtBr} \times [EtBr] = Kapp. \times [Ru(III)\ complex] \quad (4)$$

where $K_{EtBr}$ ($1.0 \times 10^7$ $M^{-1}$) is the DNA binding constant of EtBr, the concentration of EtBr is 10 μM, and [complex] is the concentration of the compound used to obtain at 50% decrease in the fluorescence intensity of EtBr.

*4.6.3. Viscosity Measurements*

Viscosity measurements were carried out using an Ubbelohde viscometer maintained in a thermostatic water bath at temperature of 30.0 ± 0.1 C. In order to minimize complexities arising from CT-DNA flexibility, CT-DNA samples with an approximate average length of 200 base pairs were prepared by sonication.[60] The DNA concentration was held constant (25 μM) and the concentration of Ru(III) complexes gradually increased. Flow time was measured with a digital stopwatch. Each sample was measured three times and an average flow time was calculated. The relative viscosities for CT-DNA in the absence and presence of the complex were calculated from the ratio $\eta = (t\text{-}t\ t_0)/t_0$, where t is the observed flow time of the solution containing DNA and $t_o$ is that of Tris -HCl buffer alone. The data are presented as $(\eta/\eta_0)^{1/3}$ versus the binding ratio of [Ru(III) complex]/[CT-DNA],[61] where η is the viscosity of the CT-DNA in the presence of the compounds and $\eta_o$ is the viscosity of the DNA alone.

*4.7. pUC19 DNA Cleavage Studies*

Supercoiled (SC) pUC19 plasmid DNA Form I in 50 mM Tris-HCl/50 mM NaCl buffer (pH 7.2) is used for investigation the DNA cleaving ability of Ru(III) complexes (1-3) by gel electrophoresis. 2μL of DNA (10μM) is treated with Ru(III) complex (30 μM) and followed by dilution with the Tris-

HCl buffer to a total volume of 20 μL. After incubation for 1 h at 37 ºC, the resulting solutions were electrophoresed for 2 h at 40 V in presence of a loading buffer containing 25% bromophenol blue, 0.35% xylene cyanol, 30% glycerol (3 μL). For monitoring the cleavage of DNA, the gel was visualized by photographing the fluorescence of intercalated ethidium bromide under a UV Transilluminator Spectroline™ TE-312S.[62] The cleavage efficiency was measured by determining the ability of the complex to convert the super coiled (SC) DNA to nicked circular form (NC) and linear form. The extent of cleavage of pUC19 was determined by measuring the intensity of the bands using AlphaImager HP Imaging System (110V) by ProteinSimple.

*4.8. Antiproliferative Activity Evaluation (MTT Assay)*

Two human cancer cell lines HeLa (cervical carcinoma) and MCF-7 (breast carcinoma) were obtained from National Cancer Institute, Cairo university. Cell lines were grown in DMEN (Dulbecco's modified Eagle's medium) supplemented with 10% heat-inactivated fetal bovine serum, 1% L-glutamine, HEPES buffer and 50 μg/ml gentamycin at 37 °C in a humidified atmosphere of 5% $CO_2$ and were sub-cultured two times a week. Standard 3-(4,5-dimethylthiazole)-2,5-diphenyltetraazolium bromide (MTT) assay procedures were used[63] to estimate the capacity of tested Ru(III) complexes to interfere with the growth of HCT-116 and MCF-7 cell lines. HCT-116 and MCF-7 cell lines with a 5 × $10^4$-$10^5$ cell/well were precultured into 96-well microtiter plates for 24 h at 37 °C. Cis-platin, Ru(III) complexes dissolved in the culture medium with 1%DMSO were added in micro wells containing the cell culture at final concentrations of 0, 1.56, 3.125, 6.25, 12.5, 25 and 50 μM. Then each well was loaded with 10 μL MTT solution (5 mg $mL^{-1}$ in phosphate buffer saline, pH = 7.4) for 4 h at 37 °C. Control wells contained supplemented media with 1% DMSO. The insoluble formazan was dissolved in 100 μL DMSO, and the cell viability was determined by recording the optical density (OD) of each well was measured at 570 nm a Bio-Rad 680 microplate reader (Bio-Rad, USA). with an ELIZA microplate reader (Meter Tech. R 960, USA). of each well at 570 nm using a Bio-Rad 680 microplate reader (Bio-Rad, USA). All experiments were performed in triplicate, and the percentage of cell viability was calculated according to the following eq (5):

$$\text{Cell viability } \% = \frac{\text{OD}_{(\text{Sample})}}{\text{OD}_{(\text{control})}} \times 100 \quad (5)$$

The $IC_{50}$ value is the concentration of thymoquinone required to produce 50% inhibition of cell growth. was calculated using the linear fit equation of the linear part of the cytotoxicity graphs (cell viability versus concentration) for each compound. The values of $IC_{50}$ were used for comparison of the cytotoxicity and chemotherapeutic characteristics among the synthesized compound. The morphological examination was performed with a Nikon ECLIPSE Ti and phase contrast images were obtained by Nikon Digital Sightds Fi1 (Nikon Corporation). The medium was removed, and the wells were washed with 200 μL phosphate buffered saline (PBS) per well. After removing the medium and PBS, the plates were centrifuged at 2500 rpm for 10 min. One hundred microliter buffer containing 0.1 M sodium acetate (pH 5.0), 0.1% Triton X-100, and 5 mM p-nitrophenyl phosphate was added to each well, and then the plates were incubated for 1.5 h at 37 ºC. After the reactions were stopped by adding 1 M NaOH, the absorbance was read at 405 nm by Victor3 (PerkinElmer). Experiments were conducted in triplicate (three independent experiments).

## Supplementary Information

Supporting information comprises entire FT-IR and ESI Mass spectral data of complexes.

## References

1 Jakupec M.A., Galanski M, Arion V.B., Hartinger C.G., and Keppler B.K. (**2008**) Antitumour metal compounds: more than theme and variations. *Dalton Trans.* 2, 183-194.

2 Nehru S., Veeralakshmi S. Kalaiselvam S. David S.P.S. Sandhya J., and Arunachalam S. (**2020**) Protein binding and antioxidant studies of diimine based emissive surfactant-ruthenium(II) complexes. *J. Biomol. Struct. Dyn.* Accepted Manuscript (DOI: 10.1080/07391102.2020.1733664).

3 Bruijnincx P.C., and Sadler P.J. (**2008**) New Trends for Metal Complexes with Anticancer Activity. *J. Curr. Opin. Chem. Biol.,* 12 (2), 197-206.

4 Tripathi L., Kumar P., and Singhai A.K. (**2007**) Role of chelates in treatment of cancer. *Indian J. Cancer,* 44 (2), 62-71.

5 Markman M. (**2003**) Toxicities of the platinum antineoplastic agents. *Expert. Opin. Drug Saf.,* 2 (6) 597-607.

6 Dasari S., and Tchounwou P.B. (**2014**) Cisplatin in Cancer Therapy: Molecular Mechanisms of Action. *Eur. J. Pharmacol.,* 740, 364-378.

7 Sankarganesh M., Raja J.D., Revathi N., Solomon R.V., and Kumar R.S. (**2019**) Gold(III) complex from pyrimidine and morpholine analogue Schiff base ligand: Synthesis, characterization, DFT, TDDFT, catalytic, anticancer, molecular modeling with DNA and BSA and DNA binding studies. *J. Mol. Liq.,* 294, 111655-111665.

8 Ahamad M.N., Iman K., Raza M.K., Kumar M., Ansari A., Ahmad M., and Shahid M. (**2020**) Anticancer properties, apoptosis and catecholase mimic activities of dinuclear cobalt(II) and copper(II) Schiff base complexes. *Bioorg. Chem.,* 95, 103561-103575.

9 Keypour H., Ansari N., Mahmoudabadi M., Karamian R., Farida S.H.M., Moghadam M.E., and Gable, R.W. (**2020**) Mn(III), Zn(II) and Pt(II) macroacyclic complexes: synthesis, X-ray structures, anticancer and antioxidant activities. *Inorg. Chim. Acta,* 509, 119705-119714.

10 Abdel Aziz A.A., and Sayed M.A. (**2020**) Some novel rare earth metal ions complexes: Synthesis, characterization, luminescence and biocidal efficiency. *Anal. Biochem.,* 598, 113645.

11 Kostova I. (**2006**) Ruthenium complexes as anticancer agents. *Curr. Med. Chem.,* 13 (9), 1085-1107.

12 Scintilla S., Brustolin L., Gambalunga A., Chiara F., and Fregona D. (**2016**) Ru(III) anticancer agents with aromatic and non-aromatic dithiocarbamates as ligands: Loading into nanocarriers and preliminary biological studies. *J. Inorg. Biochem.,* 165, 159-169.

13 Sahyon H.A., El-Bindary A.A., Shoair A.F., and Abdellatif A.A. (**2018**) Synthesis and characterization of ruthenium(III) complex containing 2-aminomethyl benzimidazole, and its anticancer activity of in vitro and in vivo models. *J. Mol. Liq.,* 255, 122-134.

14 Gramni L., Vukea N., Chakraborty A., Samson W.J., Dingle L.M.K.,. Xulu B., Mare J-A., Edkins A.L., and Booysen I.N. (**2019**) Anticancer evaluation of ruthenium(III) complexes with N-donor ligands tethered to coumarin or uracil moieties. *Inorg. Chim. Acta,* 492, 98-107.

15 Askari B., Rudbari H. A., Micale N., Schirmeister T., Maugeri, A. and Navarra M. (**2019**) Anticancer study of heterobimetallic platinum(II)-ruthenium(II) and platinum(II)-rhodium(III) complexes with bridging dithiooxamide ligand. *J. Organomet. Chem.* 900, 120918-120926.

16 Abouzayed F.I., Emam S.M., and Abouel-Enein S.A. (**2020**) Synthesis, characterization and biological activity of nano-sized Co(II), Ni(II), Cu(II), Pd(II) and Ru(III) complexes of tetradentate hydrazone ligand. *J. Mol. Struct.,* 1216, 128314-128325.

17 Pradhan A.K., and Mondal P. (**2020**) Quantum chemical investigation on the interaction of cysteine and DNA purine bases with aquated ruthenium(III) anticancer drug (ImH)[trans-$RuCl_4(Im)_2$]. *Comp. Theor. Chem.,* 1172, 112664.

18 Suchithr R., Sounthari P., Kiruthika A., Chitra S., Parameswari K., and Vijitha J. (**2016**) Ru (III) Azo Schiff Base Complexes: Synthesis, Spectral Characterization, Antimicrobial and Anticancer Studies. *Int. J. Pharm. Sci. Res.,* IJPSR 6 (3), 1283-1293.

19 Çapan A., Uruş S., and Sönmez M. (**2018**) Ru(III), Cr(III), Fe(III) Complexes of Schiff Base Ligands Bearing Phenoxy Groups: Application as Catalysts in The Synthesis of Vitamin $K_3$. *J. Saudi. Chem. Soc.,* 22 (6), 757-766.

20 Geary W.J. (**1971**) The use of conductivity measurements in organic solvents for the characterisation of coordination compounds. *Coord. Chem. Rev.,* 7, 81-122.

21 Dabbagh H.A., Teimouri A., Chermahini A.N., and Shahraki M. (**2008**) DFT and Ab initio study of structure of dyes derived from 2-Hydroxy and 2,4-Dihydroxy benzoic acids. *Spectrochim Acta A,* 69 (2), 449-4591.

22 Ünver H., Boyacıoglu B., Zeyrek C.T., Yıldız M., Demir N., Yıldırım N., Karaosmanoglu O., Sivas H., and Elmalı A. (**2016**) Synthesis, spectral and quantum chemical studies and use of (E)-3- [(3, 5-bis (trifluoromethyl)phenylimino)methyl]benzene-1, 2-diol and its Ni (II) and Cu (II) complexes as an anion sensor, DNA binding, DNA cleavage, anti-microbial, anti-mutagenic and anti-cancer agent. *J. Mol. Struct.,* 1125, 162-176.

23 Ejidike I.P., and Ajibade A. (**2016**) Ruthenium(III) Complexes of Heterocyclic Tridentate (ONN) Schiff Base: Synthesis, Characterization and its Biological Properties as an Antiradical and Antiproliferative Agent. *Int. J. Mol. Sci.,* 17 (1), 1-12.

24 Ramadan R.M., Elantabli F.M., and El-Medani S.M. (**2019**) Conversion of thiol to homodisulfide-Schiff base derivative: Synthesis, molecular structure, crystal structure and DFT studies. *J. Mol. Struct.,* 1196, 547-554.

25 Shoair A.F., El-Shobaky A.R., and Abo-Yassin H.R. (**2015**) Synthesis, spectroscopic characterization, catalytic and antibacterial studies of ruthenium(III) Schiff base complexes. *J. Mol. Liq.,* 211, 217-227.

26 Thangadurai T.D., and Natarajan K. (**2001**) Synthesis and Characterization of New Ruthenium(iii) Complexes Containing Tetradentate Schiff Bases. *Synth. React. Inorg. Met-Org. Chem*., 31 (4), 549-567.

27 İspir E., Kurtoğlu M., and Toroğlu S. (**2006**) The $d^{10}$ Metal Chelates Derived from Schiff Base Ligands Having Silane: Synthesis, Characterization, and Antimicrobial Studies of Cadmium(II) and Zinc(II) Complexes. *Synth. React. Inorg. Met-Org. Chem*., 36 (8), 627-631.

28 Thangadurai T.D., and Ihm S.K. (**2005**) Ruthenium(II) Complexes Derived from Substituted Cyclobutane and Substituted Thiazole Schiff Base Ligands: Synthetic, Spectral, Catalytic and Antimicrobial Studies. *Synth. React. Inorg. Met-Org. Chem.,* 35 (6), 499-507.

29 Manjunath M., Kulkarni A.D., Bagihalli G.B., Malladi S., and Patil S.A. (**2017**) Bio-important antipyrine derived Schiff bases and their transition metal complexes, synthesis, spectroscopic characterization, antimicrobial, anthelmintic and DNA cleavage investigation. *J. Mol. Struct.,* 1127, 314-321.

30 Buldurun K., Turan N., Savcı A., and Çolak N. (**2019**) Synthesis, structural characterization and biological activities of metal(II) complexes with Schiff bases derived from 5-bromosalicylaldehyde: Ru(II) complexes transfer hydrogenation. *J. Saudi Chem. Soc.,* 23 (2), 205-214.

31 Khan M.M.T., Srinivas D., Kureshy R.I., and Khan N.H. (**1990**) Synthesis, Characterisation and EPR Studies of Stable Ruthenium(III) Schiff Base Chloro and Carbonyl Complexes. *Inorg. Chem.,* 29 (120), 2320-2326.

32 Thangadurai T.D., Gowri M., and Natarajan K. (**2002**) Synthesis and Characterisation Of Ruthenium(iii) Complexes Containing Monobasic Bidentate Schiff Bases And Their Biological Activities. *Synth. React. Inorg. Met-Org. Chem.,* 32 (2), 329-343.

33 Aly S.A. (**2018**) Physico-chemical study of new ruthenium(III), Pd(II) and Co(II) complexes, DNA binding of Pd(II) complex and biological applications. *J. Rad. Res. App. Sci.,* 11 (3), 163-170.

34 Patel M.N., Gandhi D.S., Parmar P.A., and Joshi H.N. (**2012**) DNA-binding and cleavage activity of polypyridyl ruthenium(II) complexes. *J. Coord. Chem.,* 65 (11), 1926-1936.

35 Shobana S., Subramaniam P., Mitu L., Dharmaraja J., and Narayan S.A. (**2015**) Synthesis, structural elucidation, biological, antioxidant and nuclease activities of some 5-Fluorouracil–amino acid mixed ligand complexes. *Spectrochim. Acta A,* 134, 333-344.

36 Abd-Elzar M.M. (**2001**) Spectroscopic Characterization of Some Tetradentate Schiff Bases and Their Complexes with Nickel, Copper and Zinc. *J. Chin. Chem. Soc.,* 48 (2), 153-158.

37 Sathiyaraj S., Butcher R.J., and Jayabalakrishnan C. (**2013**) DNA interaction and cytotoxicity studies of ruthenium(III) complexes containing 3-(benzothiazol-2-yliminomethyl)-naphthalen-2-ol ligand. *J. Coord. Chem.,* 66 (4), 580-591.

38 Alonso, A., Almendral, M. J., Curto, Y., Criado, J.J., Rodríguez, E., and Manzano, J.L. (**2007**) *New Fluorescent Antitumour Cisplatin Analogue Complexes. Study of the Characteristics of their Binding to DNA by Flow Injection Analysis.* J. Fluoresc., 17 (4), 390-400.

39 Pandya S.B., Patel U.H, and Chaudhary K.P., Socha B.N., Patel N.J., and Bhatt B.S. (**2019**) DNA interaction, cytotoxicity and molecular structure of cobalt complex of 4-amino-N-(6-chloropyridazin-3-yl) benzene sulfonamide in the presence of secondary ligand pyridine. *App. Organomet. Chem.,* 33 (12), e5235.

40 Sun J., Hao H., Lin H., Liu X., Zhong D., and Chen W. (**2012**) Synthesis and Crystal Structure of a New Ru(II) Complex With Dicationic 2,2′-Dipyridyl Derivatives as Ligand. *Synth. React. Inorg. Met-Org. Chem.,,* 42 (6), 801-804.

41 Reinert K,E, (**1973**) DNA stiffening and elongation caused by the binding of ethidium bromide. *Biochim. Biophys.* Acta, 319, 135-139.

42 Gao F., Chao H., Zhou F., Yuan Y.X., Peng B., and Ji L.N. (**2006**) DNA interactions of a functionalized ruthenium(II) mixed-polypyridyl complex $[Ru(bpy)_2ppd]^{2+}$. *J. Inorg. Biochem.,* 100 (9), 1487-1494.

43 Ramana N., Sobhaa S., T and hamaraichelvan A. (**2011**) A novel bioactive tyramine derived Schiff base and its transition metal complexes as selective DNA binding agents. *Spectrochim. Acta A,* 78 (20), 888-898.

44 Muralisankar M., Haribabu J., Bhuvanesh N.S.P., and Karvembu R., and Sreekanth A. (**2016**) Synthesis, X-ray crystal structure, DNA/protein binding, DNA cleavage and cytotoxicity studies of N (4) substituted thiosemicarbazone based copper (II)/nickel (II) complexes. *Inorg. Chim. Acta,* 449 (3), 82-95.

45 Ejidike I.P., and Ajibade P.A. (**2015**) Synthesis, characterization, and in vitro antioxidant and anticancer studies of ruthenium(III) complexes of symmetric and asymmetric tetradentate Schiff bases. *J. Coord. Chem.,* 68 (14), 2552-2564.
46 Sáez R., Lorenzo J., Prietoc M.J., Font-Bardia M., Calvet T., Omeñaca N., Vilaseca M., and Moreno V. (**2014**) Influence of $PPh_3$ moiety in the anticancer activity of new organometallic ruthenium complexes. *J. Inorg. Biochem,.* 136, 1-12.
47 Jeffery G.H., Bassett J., Mendham J. (**1989**) Vogel's Textbook of Quantitative Chemical Analysis. 5th Ed, John Wiley & Sons, New York.
48 Fadeeva V.P., Vershinin V.I., and Kuzmina E.A. (**2008**) Determination of sulfur in organic compounds using a barium-selective electrode. *J. Anal. Chem.,* 63 (8), 775-778.
49 Earnshaw A. (**1986**) *Introduction to Magnetochemistry*, Academic Press, London.
50 Abdel Aziz A.A., Seda S.H. (**2015**) A novel fluorescent Optode for recognition of $Zn^{2+}$ ion based on N,N'-bis-(1-hydroxypheylimine)2,5-thiophenedicarobxaldehyde (HPTD) Schiff Base. *J. Fluoresc.,* 25 (6), 1711-1719.
51 Abdel Aziz A.A., and Seda S.H. (**2017**) Synthesis, structural features and biochemical activity assessment of N,N′-bis-(2-mercaptophenylimine)-2,5-thiophenedicarboxaldehyde Schiff Base and its Co(II), Ni(II), Cu(II) and Zn(II) complexes. *App. Organome. Chem.,* 31 (12), e3879.
52 Abdel Aziz A.A., El-Sayed I.S.A., and Khalil M.M.H. (**2017**) Some divalent metal(II) complexes from potentially tetradentate Schiff base N,N′-bis(2,5-thienylmethylidene)2-aminobenzoic acid: Synthesis, spectroscopic characterization and bioactivities. *App. Organomet. Chem.,* 31 (10), e3730.
53 Kumar A.P., Reddy P.R., and Reddy V.K. (**2013**) Direct and Derivative Spectrophotometric Determination of Ruthenium(III). *Int. J. Chem. Tech. Res.,* 5 (4), 1442-1447.
54 Kontogiorgis C., and Hadjipavlou-Litina D. (**2003**) Biological Evaluation of Several Coumarin Derivatives Designed as Possible Anti-Inflammatory/Antioxidant Agents. *J. Enz. Inhib. Med. Chem.,* 18 (1), 63-69.
55 Purtas S., Köse M., Tümer F., Tümer M., Gölcü A., and Ceyhan G. (**2016**) A novel porphyrin derivative and its metal complexes: Electrochemical, photoluminescence, thermal, DNA-binding and superoxide dismutase activity studies. *J. Mol. Struct.,* 1105, 293-307.
56 Wolfe A., Shimer G.H., and Meehan T. (**1987**) Polycyclic aromatic hydrocarbons physically intercalate into duplex regions of denatured DNA. *Biochemistry,* 26 (20), 6392-6396.
57 Chitrapriya N., Sathiyakamatchi T., Zeller M., Lee H., and Natarajan K. (**2011**) Synthesis, spectroscopic, crystal structure and DNA binding of Ru(II) complexes with 2-hydroxy-benzoic acid [1-(4-hydroxy-6-methyl-2-oxo-2H-pyran-3-yl)-ethylidene]-hydrazide. *Spectrochim. Acta A,* 81 (1),128-134.
58 Dewey T.G. (**1991**) *Biophysical and biochemical aspects of fluorescence spectroscopy*, Plenum, New York.
59 Patra A.K., Nethaji M., and Chakravarty A.R. (**2007**) Synthesis, crystal structure, DNA binding and photo-induced DNA cleavage activity of (S-metyl-l-cysteine)copper(II) complexes of heterocyclic bases. *J. Inorg. Biochem.,* 101 (2), 233-244.
60 Chaires J.B., Dattagupta N., and Crothers D.M. (**1982**) Studies on Interaction of Anthracycline Antibiotics and Deoxyribonucleic Acid: Equilibrium Binding Studies on Interaction of Daunomycin With Deoxyribonucleic Acid. *Biochemistry,* 21 (17), 3933-3840.
61 Li W., Jiang G.B., Yao J.H., Wang X.Z., Wang J., Han B.J., Xie Y.Y., Lin G.J., Huang H.L., and Liu Y.J. (**2014**) Ruthenium(II) complexes: DNA-binding, cytotoxicity, apoptosis, cellular localization, cell cycle arrest, reactive oxygen species, mitochondrial membrane potential and western blot analysis. *J. Photochem. Photobiol. B,* 140, 94-104.
62 Roy M., Chakravarthi B.V.S.K., Jayabaskaran C., Karande A.A., and Chakravarty A.R. (**2011**) Impact of Metal Binding on the Antitumor Activity and Cellular Imaging of a Metal Chelator Cationic Imidazopyridine Derivative. *Dalton Trans.,* 40 (18), 4855-4864.
63 Mosmann T. (**1983**) Rapid Colorimetric Assay for Cellular Growth and Survival: Application to Proliferation and Cytotoxicity Assays. *J. Immunol. Methods,* 65 (1-2), 55-63.